

This document is the Accepted Manuscript version of a Published Work that appeared in final form in ACS Applied Materials & Interfaces, copyright © American Chemical Society after peer review and technical editing by the publisher. To access the final edited and published work see <https://doi.org/10.1021/acsami.2c07423>.

Environmentally tolerant ionic hydrogel with high power density for low-grade heat harvesting

Jianhao Chen^{a,b}, Chaosheng Shi^a, Lian Wu^a, Yuchan Deng^b, Yaozhi Wang^b, Lei
Zhang^{a*}, Qiao Zhang^b, Feng Peng^{b*}, Xiaoming Tao^c, Mingqiu Zhang^d, Wei Zeng^{a*}

^a Department of flexible sensing technology, Institute of Chemical Engineering,

Guangdong Academy of Sciences, Guangzhou 510665, China

^b School of Chemistry and Chemical Engineering, Guangzhou University, Guangzhou

510006, China

^c Research Centre for Smart Wearable Systems, Institute of Textiles and Clothing, The

Hong Kong Polytechnic University, Hong Kong

^d Key Laboratory for Polymeric Composite and Functional Materials of Ministry of

Education, GD HPPC Lab, School of Chemistry and Chemical Engineering, Sun Yat-

Sen University, Guangzhou 510275, P. R. China

* Corresponding authors:

zengwei@gdcrci.com (Wei Zeng)

fpeng@gzhu.edu.cn (Feng Peng)

zhanglei@gdcrci.com (Lei Zhang)

ABSTRACT

Harvesting low-grade heat by ionic hydrogel thermoelectric generator (ITEG) into useful electricity is promising to power flexible electronics. However, the poor environmental tolerance of the ionic hydrogel limits its application. Herein, we demonstrate the ITEG with high thermoelectric properties, as well as excellent capabilities of water retention, freezing resistance, and self-regeneration. The obtained ITEG can maintain the original water content at ambient conditions (302 K, 65% RH) for 7 days and keep unfreezing at low temperature (253 K). It can even be self-regenerated and recovered to its original state after a water loss in high temperature conditions. Furthermore, a high ionic Seebeck coefficient of 11.3 mV K^{-1} and an impressive power density of 167.90 mW m^{-2} are achieved under a temperature difference of 20 K. A high-power density of 60.00 mW m^{-2} can also be maintained even at 258 K. After drying and re-generation, ITEG-re even exhibits a higher ionic Seebeck coefficient of 11.8 mV K^{-1} . Successful lighting of LED and charging of capacitors demonstrate the great potential of ITEG to provide continuous energy supply for powering flexible electronics.

Keywords: low-grade heat, flexible electronics, environmental tolerance, self-regeneration, ionic hydrogel thermoelectric generator

Introduction

Flexible electronics have attracted more and more attention due to excellent flexibility, portability, biocompatibility, and broad application prospects¹⁻¹² in the area of health monitoring,¹³⁻¹⁵ electronic skin,¹⁶⁻¹⁹ artificial intelligence and so on,²⁰ which have a profound impact on people's lives. As frequent charging is inconvenient for applications such as health monitoring, it is urgent to develop a facile and efficient energy harvesting method for flexible equipment. For the continuous work of flexible electronics, effective efforts have been devoted, including triboelectric nanogenerator,^{21, 22} solar cells²³ and piezoelectric nanogenerator.²³⁻²⁵ However, these devices require external kinetic or solar energy input, making it difficult to provide continuous power supply. Thermoelectric generator (TEG) can convert low-grade energy in the environment into electricity for long periods of time without additional power, which is expected to achieve continuous power supply for flexible electronics.²⁶⁻³⁴ An output power in the orders of mini-watts from a TEG which works at near room temperature is much desirable for the applications of waste heat utilization such as in wearable microelectronics, IoT and the self-powered sensors.

New high-performance flexible thermoelectric materials must be developed to be processed via cost-effective operations at room- or low-temperature for the application in wearable electronics.³⁵ The state-of-the-art flexible thermoelectric precursor materials normally consist of inorganic semiconductors, organic binder or organic conducting polymers, most of the flexible TEGs demonstrated have a limited Seebeck coefficient and output power in a range of nW~ μ W.³⁶ Benefited from thermal diffusion, ionic

conductors possess an extraordinary ionic Seebeck coefficient. For example, Cheng et al. observed a ultrahigh Seebeck coefficient of 26.1 mV K^{-1} on an ionogels made of ionic liquids and poly(vinylidene fluoride-co-hexafluoropropylene) (PVDF-HFP), which is attributed to the ion-dipole interaction between PVDF-HFP and ionic liquids.³⁷ Recently, a high Seebeck coefficient of 17 mV K^{-1} has been obtained through the synergistic effect of thermogalvanic and thermodiffusion by Han's group.³⁸ In our recent work, we also achieved a ionic Seebeck coefficient of 11.5 mV K^{-1} in a double network hydrogel by volume difference of ions.¹ Unlike electronic conductors, these large ionic Seebeck coefficients of the ionic conductors are due to the accumulation of cations at the cold side, resulting in a thermoelectric voltage similar to that of capacitors.²⁹

Although the above ionic Seebeck coefficients of the ionic conductor based TEGs are outstanding, it is still desirable to further raise the ionic conductivity and output power of these TEGs. Furthermore, it is inevitable that water loss occurs at high temperature or even at room temperature due to the large amount of water contained in ionic hydrogel, which severely limits their practicability in the thermoelectric field. On the other hand, ionic hydrogels are prone to freeze at low temperature, leading to a lower ionic conductivity, which adversely affects the heat-to-electrical conversion efficiency. The ionic hydrogel based TEGs are new comers, which show some promises in high ionic Seebeck coefficients but fail to offer environmental tolerance as well as a high TE performance. The impacts of environmental tolerance on their output performance have remained elusive. So far very few studies have paid attention to the environmental

tolerance of ionic hydrogel based thermoelectric generator, although it is very important in practical applications.³⁹⁻⁴¹

Herein, we experimentally demonstrate an ionic hydrogel thermoelectric generator (ITEG) through a simple solvent displace method. This ITEG presents an impressive ionic Seebeck coefficient of 11.3 mV K^{-1} . Simultaneously, it can remain almost 100% water retention rate under the environment of 302 K and 65% RH for over 7 days, which shows an outstanding environmental tolerance. Interestingly, benefited from the high hydration of LiCl, the ITEG can recover to the original state by absorbing water directly from the ambient air. Furthermore, after a drying-regeneration cycle, the ITEG still shows an excellent thermoelectric performance with an ionic Seebeck coefficient of 11.8 mV K^{-1} , which is closed to the initial value. By connecting six ITEGs in series, the ITEG system successfully lights the LED lamp at a temperature difference (ΔT) of 40 K. Besides, charging capacitors of different capacities has proved the great application prospect of the ITEG.

Result and discussion

The environmentally tolerant ITEG was prepared by a simple solvent displace method as shown in Fig. S1. Polyacrylamide (PAAm) was selected as a polymer network and the ITEG was obtained by soaking PAAm in LiCl solution. The SEM images show that PAAm has a porous structure that provides a large number of ion migration channels (Fig. S2). From the attenuated total reflectance-Fourier-transform infrared (ATR-FTIR) spectroscopy (Fig. S3), the PAAm hydrogel exhibits a carbonyl

group stretching vibration at 1653 cm^{-1} and an amino group stretching vibration at 3180 cm^{-1} . The disappearance of C=C stretching vibration at 1606 cm^{-1} of AAm monomer in the FTIR spectrum of PAAm indicates the successful polymerization of the AAm monomer into PAAm. Through the introduction of highly hydrate LiCl salt, the ITEG was endowed with high water retention and good frosting resistance. According to previous reports, the dissociated Li^+ and Cl^- could bind 4 and 6 water molecules in aqueous solution, respectively, thus destroying the interactions between water molecules.⁴² After losing water at a high temperature, it can directly absorb the water in the air and restore to the original state, making it possible to be applied in some extreme environment.

On account of the easy water loss of ionic hydrogel in air, it is difficult for ITEG to be continuously applied in practice. The strong interactions between Li^+/Cl^- and water molecules make it possible to retain water in LiCl based ionic hydrogel. As shown in Fig. 1a-c, the pure ITEG without LiCl loses almost 33% of its original mass after 12 hours at 302 K and 65% RH. In contrast, the ITEGs, containing 10% and 30% LiCl, retain nearly 68% and 100% of their original mass after being exposed in the same condition for 7 days, respectively, which could be attributed to the strong hydration of the LiCl. Excellent water retention capability ensures the durable availability of ITEG in the collection of low-grade thermal energy into electrical energy.

The designed ITEG is also effective at powering flexible electronics under extremely cold conditions. However, ionic hydrogel always freezes at low temperatures due to the formation of infinite hydrogen bonds between water molecules, which hinders its

application. According to previous reports,^{43, 44} as LiCl dissolved with a large number of water molecules, hydrogen bonds between water molecules are broken and the formation of ice crystals is effectively inhibited. As shown in Fig. 1d, with the introduction of LiCl, the ITEG exhibits good freezing resistance at 253 K. DSC was used to further investigate the effect of LiCl concentrations on the freezing resistance of ITEG (Fig. 1e). DSC analysis of the blank sample without LiCl shows that there are two endothermic peaks corresponding to the freezing of free water and bound water in the ITEG. At a LiCl concentration of 10%, there is an exothermic peak at 233 K, indicating the occurrence of frozen water. As the concentration of LiCl increases to 30%, it can be seen that there is no endothermic peak in the range of 203 K to 298 K, indicating that there is no frozen water in the ITEG. Interestingly, according to the stress-strain curves (Fig. 1f), the ITEG could maintain excellent stretchability (elongation at break is 480%) even with a high LiCl concentration of 30%, showing enormous potential in the flexible electronics field.

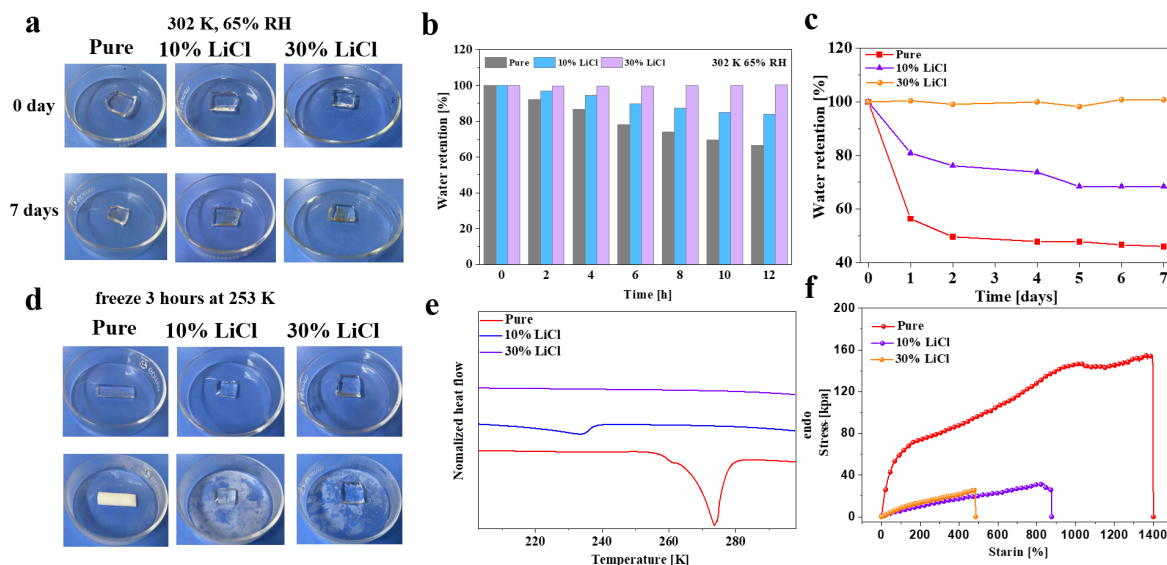


Figure 1. (a) Images of pure, 10% and 30% LiCl-based ionic hydrogels at 302 K and 65% RH for 7 days. Water retention rates of pure, 10% and 30% LiCl-based ionic hydrogel at 302 K and 65% RH for (b) 12 hours and (c) 7 days. (d) Images of pure, 10% and 30% LiCl-based ionic hydrogel at 253 K for 3 hours. (e) DSC heating curves and (f) Stress and strain curves of pure, 10% and 30% LiCl-based ionic hydrogels.

Even the addition of high concentration of LiCl reduces the vapor pressure of the ITEG so that it can keep the original state at room temperature, the ITEG still cannot maintain 100% water content under high temperature and drying conditions. To investigate the self-regeneration of the ITEG, the ITEG was dried at 333 K and regenerated at the ambient environment. Similar to the principles of water retention and anti-freeze, when ITEG is dried and loses water, the surface vapor pressure of the dehydrated ITEG is lower than that of the surrounding environment.^{43, 45} Therefore, the dehydrated ITEG will spontaneously absorb water from the air until the surface vapor pressure of ITEG and the surrounding environment reach equilibrium. As shown in Fig. 2a, the ITEG lost a considerable amount of water after being dried at 333 K for 2 hours

and restored to the original state at the ambient environment (302 K, 65% RH). In contrast, other chlorine salts, like NaCl, KCl cannot be restored to their original state after water loss (Fig. S4). Even after several drying-regeneration cycles, the ITEG can still recover to its original state (Fig. 2b), demonstrating that the evaporation and regeneration processes are invertible and repeatable. Due to the high hygroscopicity of LiCl, the dehydrated ITEG can directly absorb moisture from the air and recover to its original state. Therefore, the water content of ITEG can be regulated through this controllable self-regeneration process. Furthermore, the ionic hydrogel maintains a similar elongation at break to the original sample after self-regeneration, demonstrating that it retains good stretchable properties (Fig. 2c).

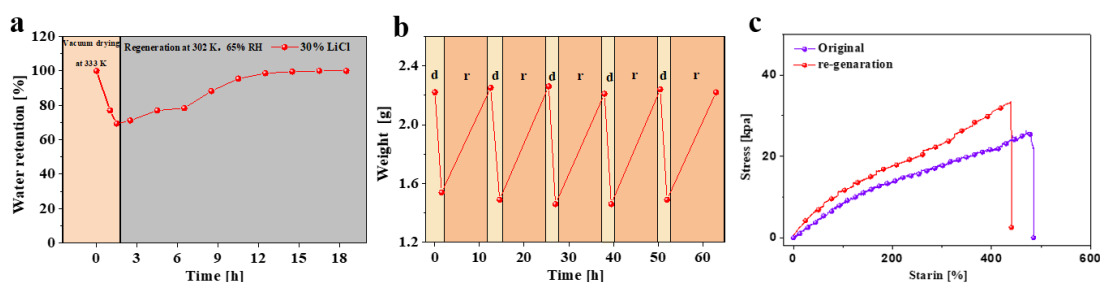


Figure 2. (a) Water retention of 30% LiCl-based ionic hydrogel during vacuum drying at 333 K and regeneration at 302 K, 65% RH. (b) The drying-regeneration cycles at the same time. (c) Stress and strain curves before and after self-regeneration of 30% LiCl-based ionic hydrogel.

The as-prepared ionic hydrogel based TEG is essentially a capacitor based on the thermal diffusion effect, because the ions cannot transmit through the electrode to an external circuit. The corresponding mechanism is shown in Fig. S5. In the initial state, Li^+ and Cl^- are evenly dispersed in the ITEG. When there is a ΔT between the two

electrodes, Li^+ will migrate to the cold side due to the Soret effect which refers to the phenomenon of ions migration in an electrolyte due to thermal diffusion. Li^+ is smaller in volume and has greater relative mobility than Cl^- . Eventually, high concentrations of Li^+ and Cl^- were collected at the cold side and hot side, respectively, resulting in a thermoelectric voltage. Ionic Seebeck coefficient is used to define the thermoelectric properties of the ITEG. As shown in Fig. S6, after a period of hot charging, the open circuit voltage reaches saturation and remains stable. The open circuit voltage of the ITEG was tested under different ΔT , and a high ionic Seebeck coefficient of 11.3 mV K^{-1} was obtained from the fitting results (Fig. 3a). With the increase of ΔT , the corresponding open circuit voltage increases linearly. While in the absence of ΔT , the open circuit voltage is approximately zero. Moreover, the output power density of the ITEG was shown in Fig. 3b. When the temperature of the hot side is fixed at 318 K, according to the current density-output voltage and current density-power density curves, the ITEG shows a short-circuit current density of 1.11 A m^{-2} and an instantaneous maximum output power density of 57.30 mW m^{-2} under a ΔT of 10 K. As for the voltage-current curve, which shows a nonlinear curve due to the low ion mobility and the changing internal resistance during the power output of the device. As the ΔT increases to 20 K, the ITEG shows a short-circuit current density of 1.62 A m^{-2} and an instantaneous maximum output power density of 167.90 mW m^{-2} . Compared to some recently reported ion thermoelectric generators, the power density of our ITEG is more than an order of magnitude higher (Table S1, Supporting information). The output

voltage and instantaneous output power density increase linearly as the ΔT increases in the temperature range of 258~318 K.

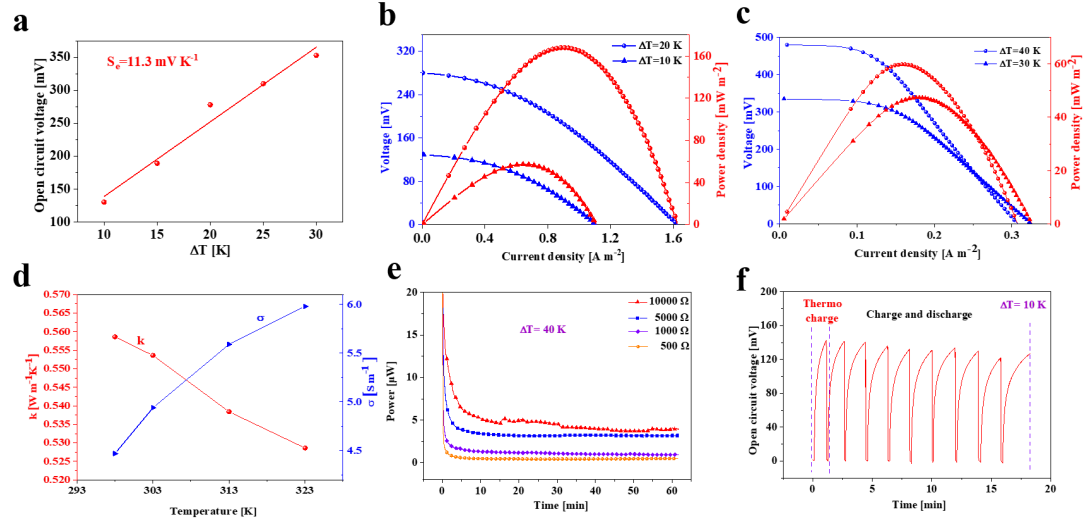


Figure 3. (a) Dependence of the open circuit voltage of ITEG on the temperature difference from 10 to 30 K. (b) voltage-current density and power density-current density curves under the temperature difference of 10 and 20 K. The hot side is fixed at 318 K (c) Voltage-current density and power density-current density curves under the temperature difference of 30 and 40 K. The hot side is fixed at 298 K and the cold side is 258 and 268 K, respectively. (d) Thermal conductivity and ionic conductivity of ITEG under 298-323 K. (e) Power of the discharge process at the different external resistors. (f) Cyclic thermal charge-discharge test.

Similarly, to indicate the output power of the ITEG at low temperatures, the hot side of the ITEG is fixed at 298 K and the cold side is set at 258 and 268 K respectively. As shown in Fig. 3c, the short-circuit current density reaches 0.31 A m^{-2} and the instantaneous output power density is 60.00 mW m^{-2} under a ΔT of 40 K. The reason for the lower short-circuit current density and instantaneous power density is that the

declining ionic conductivity at low temperatures increases the internal resistance of the ITEG. Nevertheless, the ITEG still maintains a good output power density even the cold side decreases to 258 K. This wide temperature range ionic hydrogel based thermoelectric generator indicates a great potential for thermoelectric applications at low temperatures.

The thermal conductivity of the ITEG was measured by the Hot Disk method. As Fig. 3d depicts, the thermal conductivity decreases from 0.5586 to 0.5286 W m⁻¹ K⁻¹ with increasing temperature in the range of 298-323 K. Meanwhile, the ionic conductivity of the ITEG was measured by AC impedance spectroscopy. Instead of a semicircle, a straight line is seen in the high frequency region of the Nyquist plots, which is consistent with the results of gels in our previous work (Fig. S7).¹ The ionic resistance of the ITEG is obtained by intercepting the straight line. The calculated ionic conductivity of the ITEG is 4.47-5.98 S m⁻¹ in the range of 298-323 K (Fig. 3d). The ion migration rate in the ITEG increases with the rising temperature, which enhances the ionic conductivity of the ITEG.

The output stability of the ITEG was further investigated to prove that the ITEG can be applied for a long time. As shown in Fig. 3e, when the ITEG is connected in series with external different resistors to form a closed loop, the output power decays rapidly from the maximum to a stable value, forming a stable power output operation mode and remaining stable for 60 minutes. The energy density with different external resistors is calculated as shown in Fig. S8. Corresponding energy density to an external resistance of 10000 Ω reaches 172.1 J m⁻². Moreover, the heat-to-electrical efficiency (η) relative

to Carnot efficient (η_c) for the ITEG could expressed by the following equation: $\eta_r = \frac{\eta}{\eta_c} = \frac{t_{dis}}{t_{ch}} \frac{P_{ave}}{\Delta T^2} T_H \frac{d}{\lambda}$, where η_r , t_{dis} , t_{ch} , P_{ave} , d , λ are the Carnot-relative efficiency, discharge time, thermal charge time, average long-time power density and thermal conductivity, respectively⁴⁶. As shown in Fig. S9, ITEG has the highest thermoelectric conversion efficiency of 0.016% to 10000 Ω external resistor. Further, to verify that this ionic hydrogel based thermoelectric material is not a disposable power source, a cyclic charge-discharge test was performed on the ITEG. The cold side and hot side are fixed at 308 K and 318 K, respectively ($\Delta T = 10$ K). Fig. 3f reveals that the ITEG gradually charges from 0 V to its maximum open circuit voltage during the thermal charging process. Subsequently, the output voltage of the ITEG decays to 0 in a few seconds through an external circuit. When the external circuit is disconnected, the ITEG regains the maximum output voltage after 90 seconds. As the number of cycles increases, it takes longer time for the ITEG to return to the maximum output voltage. This phenomenon is probably caused by the polarization of the electrodes, which is consistent with the results we have reported earlier.¹

The self-regeneration capability of the dehydrated ITEG endows the ITEG with a very high practical potential. Therefore, the thermoelectric properties of the ITEG after self-regeneration are evaluated. On this count, we placed the high-temperature dried ITEG at room temperature and humidity (302 K, 65% RH) for a period of 8 hours, and it returned to its original state and was named as ITEG-re. Similarly, the open circuit voltages of the ITEG-re under different ΔT were measured. As shown in Fig. 4a, the fitting result shows that the ITEG-re has an ionic Seebeck coefficient of 11.8 mV K⁻¹,

which is close to that of the pristine ITEG. This result shows that the regenerated ITEG can retain good thermoelectric properties as high as that of the pristine ITEG. This impressive environmental tolerance and strong thermoelectric performance retention make the ITEG extremely useful in practical applications. Meanwhile, the continuous output power of the ITEG was also evaluated. Fig. 4b reveals that the ITEG-re also maintains a continuous power output for 60 minutes against the external resistance of $5000\ \Omega$, which verifies its output stability. As a comparison, the change in energy density for an external resistor of $5000\ \Omega$ after self-regeneration is calculated. As shown in Fig. S10, the energy density after self-regeneration is $105.6\ \text{J m}^{-2}$, which is slightly lower than the original ($110.4\ \text{J m}^{-2}$).

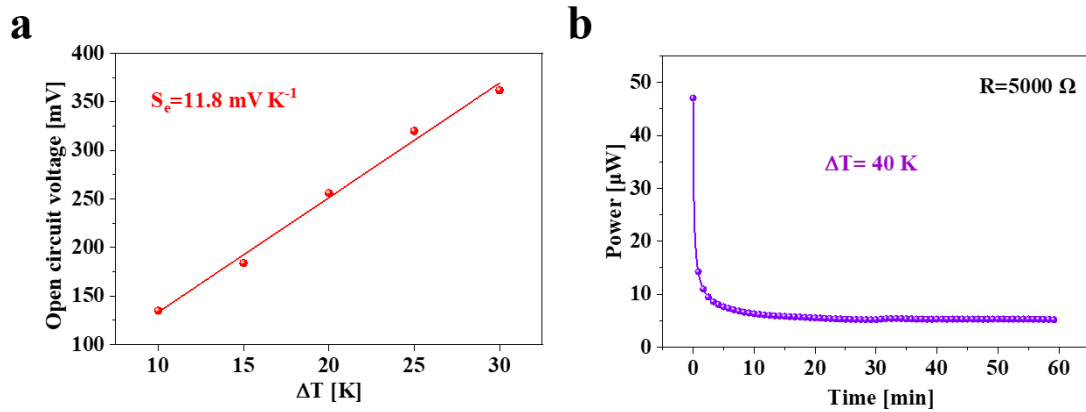


Figure 4. (a) Dependence of open circuit voltage of ITEG-re on the temperature difference from 10 to 30 K. (b) Power of the discharge process at a $5000\ \Omega$ external resistor.

To demonstrate the potential application of the ITEG in practice, the self-powered sensor of ITEG is schematically illustrated in Fig. 5a and 5c. The self-powered sensor works by transforming the external input signal into the electrical output signal, which can be driven by the ITEG directly. An external resistance R_f ($1000\ \Omega$) was selected as

the electrical signal output terminal. According to the equation, $V_f = \frac{V_0}{R+R_f} R_f$, where V_0 is the open circuit voltage of the ITEG, V_f is the load-voltage, and R is the internal resistance of the ITEG. When there is a ΔT between the electrodes of the ITEG, an open circuit voltage V_0 is generated. When an external compression strain is applied to the self-powered sensor, the internal resistance R decreases due to the shorter spacing between ions in the ITEG. As a result, the load voltage of the external resistance (V_f) increases with the enhancing of the applied compression strain. The input strain signal can be converted to the voltage change of the external resistance. As Fig. 5b depicts, when the ΔT between the two sides of the ITEG is fixed at 30 K, the load voltage of the external resistor is stable at 15.2 mV. When the ITEG is pressed, 42% and 63% compression strains are generated, resulting in an increase in the load voltage of the external resistor to 19.6 and 21.8 mV, respectively. As alternately press and release the ITEG, the load voltage of the external resistance presents a repeatable change. The corresponding input strain can be converted into the repeatable signal output of the voltage change rate. As shown in Fig. 5b, when a 63% strain is applied to the ITEG, the corresponding voltage change rate (ΔV) is 33.2%. Similarly, self-powered tensile strain sensor has been designed using the same strategy (Fig. 5c). The self-powered sensor exhibits sensitive and clear sensing signals under different degrees of stretching (Fig. 5d). This operation modes enable the ITEG self-powered sensor to harvest low grade energy for self-powered strain sensing.

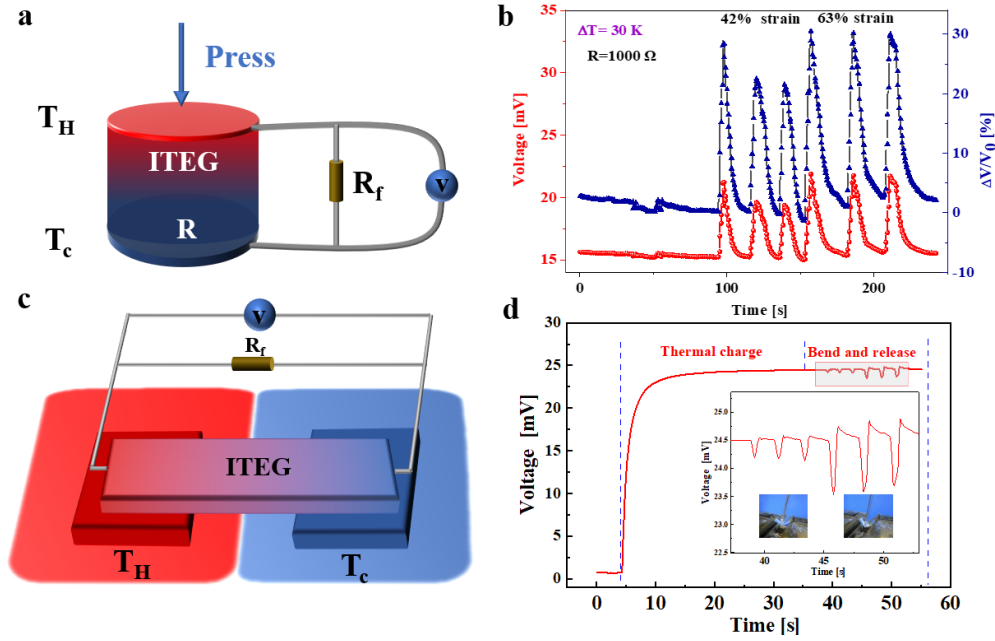


Figure 5. (a, c) Schematic structure of the ITEG self-powered sensor. (b) Load-voltage change and relative load-voltage change under different compressive strains. The height of ITEG is 15 mm, each compression value is L_0 , using $L_0/15$ (%) that is to get the compressive strain. (d) Load-voltage change under the different bending.

Furthermore, to prove the ITEG can be used in practical application, six ITEGs were connected in series with a LED (Fig. 6a). At ambient temperatures, the LED is naturally off because no thermoelectric voltage is generated. When the ITEG is given a ΔT of 40 K ($T_c = 283$ K, $T_h = 323$ K), the ions will gather at each side to generate a stable thermoelectric voltage (Fig. 6b). When the ITEGs are connected to the LED, the LED lights up and the thermoelectric voltage of the ITEGs decreases due to the electron migration in the closed loop (Fig. 6b and 6c). In addition, the ITEGs can effectively charge capacitors. As shown in Fig. 6d, the ITEGs can effectively charge up capacitors to a certain voltage value and remain stable when they are connected to a capacitor. As

for a capacitor of 220 μF , it can be charged to 1.46 V in 200 s. Therefore, ITEG is a sustainable energy source with great potential for application, not only in the power supply of flexible electronic devices but also in energy storage devices.

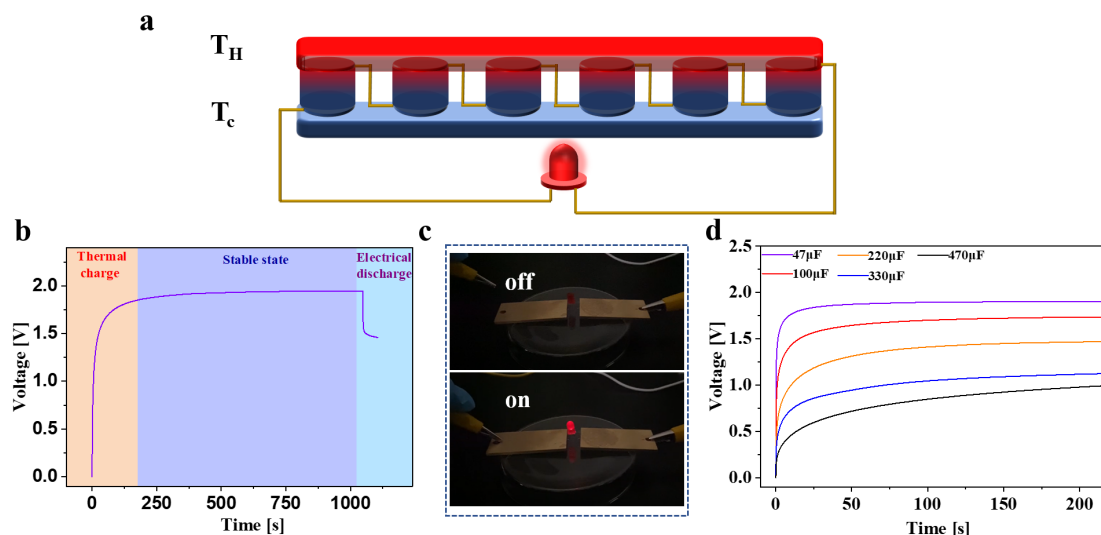


Figure 6. (a) Schematic illustration of the ITEG system. (b) The thermal charge and electrical process of the ITEG system. (c) Photos of the LED. (d) Different capacitors charging by ITEG system.

Conclusion

In summary, we demonstrate an ITEG based on PAAm/LiCl ionic hydrogel which has strong water retention, frosting resistance, and self-regeneration capability. The strong hydration of LiCl enhances the interaction between hydrogel and water, avoiding evaporation and freezing of water in ionic hydrogel. Thus, the as-prepared ITEG can harvest low-grade heat to generate a high ionic Seebeck coefficient of 11.3 mV K^{-1} and an impressive power density of 167.90 mW m^{-2} under a temperature difference of 20 K. Besides, the anti-freezing ITEG still has a relatively high-power density of 60.00 mW

m^{-2} even at a low temperature of 258 K. The ITEG-re still has an ionic Seebeck coefficient of 11.8 mV K^{-1} , close to the value of the pristine ITEG. To prove the ITEG can be used in practical situation, six ITEGs were connected in series with a LED or capacitors. The ITEG system successfully lights up LED and can charge up capacitors under the temperature difference of 40 K. This sustainable heat-to-electrical energy is expected to be used to power electronic devices and store energy.

Experimental section

Materials. Lithium chloride (LiCl,99%) and Potassium persulfate (KPS) were purchased from Aladdin (Shanghai, China). Acrylamide (AAm,99%), *N, N'*-methylene bis-acrylamide (MBAA), and *N, N, N', N'*-Tetramethylethylenediamine (TEMED,99%) were purchased from Macklin (Shanghai, China).

Preparation of the ITEG. Firstly, AAm monomers were added into deionized water and stirred in an ice bath until they are completely dissolved. And then, 200 μ L of MBAA aqueous solution (0.01g/mL) and 5 mL of KPS aqueous solution (0.01g/mL) were added while stirring for 15 min. Finally, 100 μ L of TEMED were added and stirred for 1 min. The dispersed solution was then poured into a cylindrical silicon mold (The radius and the height are both 15 mm) to polymerize naturally at room temperature for 24 hours, obtaining the PAAm hydrogel. Subsequently the PAAm hydrogel was immersed into the LiCl aqueous solution with different concentration (0, 10, and 30 wt%) for about 24 hours to ensure complete solvent exchange, thus the ITEGs were obtained.

Characterization and Measurement. Thermoelectric effects were measured using a electrochemical workstation (Chi760e) that was coupled with a temperature controller. attenuated total reflectance-Fourier-transform infrared (ATR-FTIR) spectroscopy was measured by Nicolet IS5 (ThermoFisher). DSC analysis was measured by a DSC system (TA-DSC2500). Thermal conductivity was measured by the transient plane heat

source method (TPS2500S, Sweden). The ionic conductivity was measured by AC impedance spectroscopy (Chi760e). The ionic Seebeck coefficient measurements were performed using a temperature controller: After performing the thermal charging to reach the saturation open circuit voltage, the saturation open circuit voltage as well as the temperature difference are recorded. Subsequently, the electrodes are connected at both sides through an external circuit and the voltage becomes 0 V after a period of time. The temperature difference is changed while keeping the external circuit connected. Further, the external circuit is disconnected after the next temperature difference is maintained for 40 minutes, and then the next period of thermal charging is performed and the open-circuit voltage is recorded.

Associated Content

Supporting Information

Schematic of the preparation process and chemical structure of the ITEG, SEM and ATR-FTIR analyses, mechanism of thermal voltage generation, V-t curves and EIS measurements, energy density and η_r of ITEG, comparison of power density

Author Information

Corresponding Authors

Lei Zhang- Department of flexible sensing technology, Institute of Chemical Engineering, Guangdong Academy of Sciences, Guangzhou 510665, China; Email: zhanglei@gdcri.com.

Feng Peng- School of Chemistry and Chemical Engineering, Guangzhou University, Guangzhou 510006, China; Email: fpeng@gzhu.edu.cn.

Wei Zeng- Department of flexible sensing technology, Institute of Chemical Engineering, Guangdong Academy of Sciences, Guangzhou 510665, China; Email: zengwei@gdcric.com.

Authors

Jianhao Chen- Department of flexible sensing technology, Institute of Chemical Engineering, Guangdong Academy of Sciences, Guangzhou 510665, China; School of Chemistry and Chemical Engineering, Guangzhou University, Guangzhou 510006, China

Chaosheng Shi- Department of flexible sensing technology, Institute of Chemical Engineering, Guangdong Academy of Sciences, Guangzhou 510665, China

Lian Wu- Department of flexible sensing technology, Institute of Chemical Engineering, Guangdong Academy of Sciences, Guangzhou 510665, China

Yuchan Deng- School of Chemistry and Chemical Engineering, Guangzhou University, Guangzhou 510006, China

Yaozhi Wang- School of Chemistry and Chemical Engineering, Guangzhou University, Guangzhou 510006, China

Qiao Zhang- School of Chemistry and Chemical Engineering, Guangzhou University, Guangzhou 510006, China

Xiao-Ming Tao- Research Centre for Smart Wearable Systems, Institute of Textiles and Clothing, The Hong Kong Polytechnic University, Hong Kong

Mingqiu Zhang- Key Laboratory for Polymeric Composite and Functional Materials of Ministry of Education, GD HPPC Lab, School of Chemistry and Chemical Engineering, Sun Yat-Sen University, Guangzhou 510275, P. R. China

Author Contributions

Chen, Jianhao: Conceptualization, methodology, investigation, writing-original draft, and writing-review and editing. Shi, Chaosheng: Investigation and methodology. Wu,

Lian: Investigation and methodology. Deng, Yuchan: Investigation and methodology. Wang, Yaozhi: Investigation and methodology. Zhang, Lei: Resources and writing-review and editing. Zhang, Qiao: Investigation. Peng, Feng: Methodology, supervision, funding acquisition and writing-review and editing. Tao, Xiao-Ming: Writing-review and editing. Zhang, Ming Qiu: Writing-review and editing. Zeng, Wei: Methodology, supervision, funding acquisition, project administration and writing-review and editing.

Acknowledgements

The work has been partially supported by National Natural Science Foundation of China (Grant No. 52073066, 21673080), the GDAS Project of Science and Technology Development (Grant No. 2020GDASYL-20200102028) and Science and Technology Planning Project of Guangzhou City, China (Grant No. 202102080329).

References

1. Chen, J.; Zhang, L.; Tu, Y.; Zhang, Q.; Peng, F.; Zeng, W.; Zhang, M.; Tao, X. J. N. E., Wearable Self-Powered Human Motion Sensors based on Highly Stretchable Quasi-Solid State Hydrogel. *Nano Energy* **2021**, *88*, 106272.
2. Zeng, W.; Shu, L.; Li, Q.; Chen, S.; Wang, F.; Tao, X.-M., Fiber-based Wearable Electronics: a Review of Materials, Fabrication, Devices, and Applications. *Adv. Mater.* **2014**, *26*, 5310-5336.
3. Araromi, O. A.; Graule, M. A.; Dorsey, K. L.; Castellanos, S.; Foster, J. R.; Hsu, W.-H.; Passy, A. E.; Vlassak, J. J.; Weaver, J. C.; Walsh, C. J.; Wood, R. J., Ultra-

Sensitive and Resilient Compliant Strain Gauges for Soft Machines. *Nature* **2020**, *587*, 219-224.

4. Bai, H.; Li, S.; Barreiros, J.; Tu, Y.; Pollock, C. R.; Shepherd, R. F., Stretchable Distributed Fiber-Optic Sensors. *Science* **2020**, *370*, 848-852.

5. Fuentes-Hernandez, C.; Chou, W.-F.; Khan, T. M.; Diniz, L.; Lukens, J.; Larrain, F. A.; Rodriguez-Toro, V. A.; Kippelen, B., Large-Area Low-Noise Flexible Organic Photodiodes for Detecting Faint Visible Light. *Science* **2020**, *370*, 698-701.

6. Gu, L.; Poddar, S.; Lin, Y.; Long, Z.; Zhang, D.; Zhang, Q.; Shu, L.; Qiu, X.; Kam, M.; Javey, A.; Fan, Z., A Biomimetic Eye with a Hemispherical Perovskite Nanowire Array Retina. *Nature* **2020**, *581*, 278-282.

7. Kim, H. J.; Chen, B.; Suo, Z.; Hayward, R. C., Ionoelastomer Junctions Between Polymer Networks of Fixed Anions and Cations. *Science* **2020**, *367*, 773-776.

8. Lee, S.; Franklin, S.; Hassani, F. A.; Yokota, T.; Nayeem, O. G.; Wang, Y.; Leib, R.; Cheng, G.; Franklin, D. W.; Someya, T., Nanomesh Pressure Sensor for Monitoring Finger Manipulation without Sensory Interference. *Science* **2020**, *370*, 966-970.

9. Liu, J.; Kim, Y. S.; Richardson, C. E.; Tom, A.; Ramakrishnan, C.; Birey, F.; Katsumata, T.; Chen, S.; Wang, C.; Wang, X.; Joubert, L.-M.; Jiang, Y.; Wang, H.; Fenno, L. E.; Tok, J. B. H.; Pasca, S. P.; Shen, K.; Bao, Z.; Deisseroth, K., Genetically Targeted Chemical Assembly of Functional Materials in Living Cells, Tissues, and Animals. *Science* **2020**, *367*, 1372-1376.

10. Liu, X.; Gao, H.; Ward, J. E.; Liu, X.; Yin, B.; Fu, T.; Chen, J.; Lovley, D. R.; Yao, J., Power Generation from Ambient Humidity Using Protein Nanowires. *Nature* **2020**,

578, 550-554.

11. You, I.; Mackanic, D. G.; Matsuhisa, N.; Kang, J.; Kwon, J.; Beker, L.; Mun, J.; Suh, W.; Kim, T. Y.; Tok, J. B. H.; Bao, Z.; Jeong, U., Artificial Multimodal Receptors based on Ion Relaxation Dynamics. *Science* **2020**, *370*, 961-965.
12. Yang, Z.; Huang, T.; Cao, P.; Cui, Y.; Nie, J.; Chen, T.; Yang, H.; Wang, F.; Sun, L., Carbonized Silk Nanofibers in Biodegradable, Flexible Temperature Sensors for Extracellular Environments. *ACS Appl. Mater. Interfaces* **2022**, *14*, 18110-18119.
13. Cai, G.; Wang, J.; Qian, K.; Chen, J.; Li, S.; Lee, P. S. J. A. S., Extremely Stretchable Strain Sensors based on Conductive Self-Healing Dynamic Cross-Links Hydrogels for Human-Motion Detection. *Adv. Sci.* **2017**, *4*, 1600190.
14. Zang, Y.; Zhang, F.; Di, C.-A.; Zhu, D., Advances of Flexible Pressure Sensors Toward Artificial Intelligence and Health Care Applications. *Mater. Horiz.* **2015**, *2*, 140-156.
15. Wang, X.; Gu, Y.; Xiong, Z.; Cui, Z.; Zhang, T., Silk-Molded Flexible, Ultrasensitive, and Highly Stable Electronic Skin for Monitoring Human Physiological Signals. *Adv. Mater.* **2014**, *26*, 1336-1342.
16. Sun, J.-Y.; Keplinger, C.; Whitesides, G. M.; Suo, Z., Ionic Skin. *Adv. Mater.* **2014**, *26*, 7608-7614.
17. Yi, F.-L.; Guo, F.-L.; Li, Y.-Q.; Wang, D.-Y.; Huang, P.; Fu, S.-Y., Polyacrylamide Hydrogel Composite E-Skin Fully Mimicking Human Skin. *ACS Appl. Mater. Interfaces* **2021**, *13*, 32084-32093.
18. Wang, Z.; Bu, T.; Li, Y.; Wei, D.; Tao, B.; Yin, Z.; Zhang, C.; Wu, H.,

Multidimensional Force Sensors based on Triboelectric Nanogenerators for Electronic Skin. *ACS Appl. Mater. Interfaces* **2021**, *13*, 56320-56328.

19. Liu, Y.-Q.; Zhang, J.-R.; Han, D.-D.; Zhang, Y.-L.; Sun, H.-B., Versatile Electronic Skins with Biomimetic Micronanostructures Fabricated Using Natural Reed Leaves as Templates. *ACS Appl. Mater. Interfaces* **2019**, *11*, 38084-38091.

20. Xia, S.; Song, S.; Gao, G., Robust and Flexible Strain Sensors based on Dual Physically Cross-Linked Double Network Hydrogels for Monitoring Human-Motion. *Chem. Eng. J.* **2018**, *354*, 817-824.

21. Fan, F. R.; Tang, W.; Wang, Z. L., Flexible Nanogenerators for Energy Harvesting and Self-Powered Electronics. *Adv. Mater.* **2016**, *28*, 4283-4305.

22. Cheng, B.; Niu, S.; Xu, Q.; Wen, J.; Bai, S.; Qin, Y., Griding Triboelectric Nanogenerator for Raindrop Energy Harvesting. *ACS Appl. Mater. Interfaces* **2021**, *13*, 59975-59982.

23. Kim, B. J.; Kim, D. H.; Lee, Y.-Y.; Shin, H.-W.; Han, G. S.; Hong, J. S.; Mahmood, K.; Ahn, T. K.; Joo, Y.-C.; Hong, K. S.; Park, N.-G.; Lee, S.; Jung, H. S., Highly Efficient and Bending Durable Perovskite Solar Cells: Toward a Wearable Power Source. *Energy Environ. Sci* **2015**, *8*, 916-921.

24. Park, D. Y.; Joe, D. J.; Kim, D. H.; Park, H.; Han, J. H.; Jeong, C. K.; Park, H.; Park, J. G.; Joung, B.; Lee, K. J., Self-Powered Real-Time Arterial Pulse Monitoring Using Ultrathin Epidermal Piezoelectric Sensors. *Adv. Mater.* **2017**, *29*, 1702308.

25. Wang, S.; Lin, L.; Wang, Z. L., Triboelectric Nanogenerators as Self-Powered Active Sensors. *Nano Energy* **2015**, *11*, 436-462.

26. Burton, M. R.; Mehraban, S.; Beynon, D.; Mcgettrick, J.; Watson, T.; Lavery, N. P.; Carnie, M. J., 3D Printed SnSe Thermoelectric Generators with High Figure of Merit. *Adv. Energy Mater.* **2019**, *9*, 1900201.
27. Duan, J.; Feng, G.; Yu, B.; Li, J.; Chen, M.; Yang, P.; Feng, J.; Liu, K.; Zhou, J., Aqueous Thermogalvanic Cells with a High Seebeck Coefficient for Low-Grade Heat Harvest. *Nat. Commun.* **2018**, *9*, 5146.
28. Gao, H.; Guo, B.; Song, J.; Park, K.; Goodenough, J. B., A Composite Gel-Polymer/Glass-Fiber Electrolyte for Sodium-Ion Batteries. *Adv. Energy Mater.* **2015**, *5*, 1402235.
29. Zhao, D.; Wang, H.; Khan, Z. U.; Chen, J. C.; Gabrielsson, R.; Jonsson, M. P.; Berggren, M.; Crispin, X., Ionic Thermoelectric Supercapacitors. *Energy Environ. Sci.* **2016**, *9*, 1450-1457.
30. Liang, L.; Wang, M.; Wang, X.; Peng, P.; Liu, Z.; Chen, G.; Sun, G., Initiating a Stretchable, Compressible, and Wearable Thermoelectric Generator by a Spiral Architecture with Ternary Nanocomposites for Efficient Heat Harvesting. *Adv. Funct. Mater.* **2022**, *32*, 2111435.
31. Liu, Z.; Wang, X.; Wei, S.; Lv, H.; Zhou, J.; Peng, P.; Wang, H.; Chen, G., A Wavy-Structured Highly Stretchable Thermoelectric Generator with Stable Energy Output and Self-Rescuing Capability. *Ccs Chem.* **2021**, *3*, 2404-2414.
32. Peng, P.; Zhou, J.; Liang, L.; Huang, X.; Lv, H.; Liu, Z.; Chen, G., Regulating Thermogalvanic Effect and Mechanical Robustness Via Redox Ions for Flexible Quasi-Solid-State Thermocells. *Nano-Micro Lett.* **2022**, *14*, 1-15.

33. Wang, X.; Liang, L.; Lv, H.; Zhang, Y.; Chen, G., Elastic Aerogel Thermoelectric Generator with Vertical Temperature-Difference Architecture and Compression-Induced Power Enhancement. *Nano Energy* **2021**, *90*, 106577.
34. Liang, L.; Lv, H.; Shi, X.-L.; Liu, Z.; Chen, G.; Chen, Z.-G.; Sun, G., A Flexible Quasi-Solid-State Thermoelectrochemical Cell with High Stretchability as an Energy-Autonomous Strain Sensor. *Mater. Horiz.* **2021**, *8*, 2750-2760.
35. Dresselhaus, M. S.; Chen, G.; Tang, M. Y.; Yang, R. G.; Lee, H.; Wang, D. Z.; Ren, Z. F.; Fleurial, J. P.; Gogna, P., New Directions for Low-Dimensional Thermoelectric Materials. *Adv. Mater.* **2007**, *19*, 1043-1053.
36. Chang, C.; Wu, M.; He, D.; Pei, Y.; Wu, C.-F.; Wu, X.; Yu, H.; Zhu, F.; Wang, K.; Chen, Y.; Huang, L.; Li, J.-F.; He, J.; Zhao, L.-D., 3D Charge and 2D Phonon Transports Leading to High out-of-Plane ZT in N-Type SnSe Crystals. *Science* **2018**, *360*, 778-782.
37. Cheng, H.; He, X.; Fan, Z.; Ouyang, J., Flexible Quasi-Solid State Ionogels with Remarkable Seebeck Coefficient and High Thermoelectric Properties. *Adv. Energy Mater.* **2019**, *9*, 1901085.
38. Han, C.-G.; Qian, X.; Li, Q.; Deng, B.; Zhu, Y.; Han, Z.; Zhang, W.; Wang, W.; Feng, S.-P.; Chen, G.; Liu, W., Giant Thermopower of Ionic Gelatin Near Room Temperature. *Science* **2020**, *368*, 1091-1098.
39. Li, T.; Zhang, X.; Lacey, S. D.; Mi, R.; Zhao, X.; Jiang, F.; Song, J.; Liu, Z.; Chen, G.; Dai, J.; Yao, Y.; Das, S.; Yang, R.; Briber, R. M.; Hu, L., Cellulose Ionic Conductors with High Differential Thermal Voltage for Low-Grade Heat Harvesting. *Nat. Mater.* **2019**, *18*, 608-613.

40. Cheng, H.; Yue, S.; Le, Q.; Qian, Q.; Ouyang, J., A Mixed Ion-Electron Conducting Carbon Nanotube Ionogel to Efficiently Harvest Heat from both a Temperature Gradient and Temperature Fluctuation. *J. Mater. Chem. A*. **2021**, *9*, 13588-13596.
41. Lei, Z.; Gao, W.; Wu, P., Double-Network Thermocells with Extraordinary Toughness and Boosted Power Density for Continuous Heat Harvesting. *Joule* **2021**, *5*, 2211-2222.
42. Isabel Barba, M.; Soledad Larrechi, M.; Coronas, A., Quantitative Analysis of the Hydration of Lithium Salts in Water Using Multivariate Curve Resolution of Near-Infrared Spectra. *Anal. Chim. Acta* **2016**, *919*, 20-27.
43. Sui, X.; Guo, H.; Cai, C.; Li, Q.; Wen, C.; Zhang, X.; Wang, X.; Yang, J.; Zhang, L., Ionic Conductive Hydrogels with Long-Lasting Antifreezing, Water Retention and Self-Regeneration Abilities. *Chem. Eng. J.* **2021**, *419*, 129478.
44. Ge, W.; Cao, S.; Yang, Y.; Rojas, O. J.; Wang, X., Nanocellulose/LiCl Systems Enable Conductive and Stretchable Electrolyte Hydrogels with Tolerance to Dehydration and Extreme Cold Conditions. *Chem. Eng. J.* **2021**, *408*, 127306.
45. Conde, M. R., Properties of Aqueous Solutions of Lithium and Calcium Chlorides: Formulations for Use in Air Conditioning Equipment Design. *Int. J. Therm. Scis.* **2004**, *43*, 367-382.
46. Li, Y.; Li, Q.; Zhang, X.; Deng, B.; Han, C.; Liu, W., 3D Hierarchical Electrodes Boosting Ultrahigh Power Output for Gelatin-KCl-FeCN^{4-/3-} Ionic Thermoelectric Cells. *Adv. Energy Mater.* **2022**, *12*, 2103666.

Declaration of interests

The authors declare that they have no known competing financial interests or personal relationships that could have appeared to influence the work reported in this paper.

